<Paper>

Reduction of vibration amplitude in vibration-type electricity generator using magnetic wire

Akitoshi Takebuchi, Tsutomu Yamada, and Yasushi Takemura

Department of Electrical and Computer Engineering, Yokohama National Univ.,
79-5 Tokiwadai, Hodogaya-ku, Yokohama 240-8501, Japan

A fast magnetization reversal accompanied by a large Barkhausen jump in a magnetic wire is utilized in speed sensors, rotation sensors, and other applications. This magnetization reversal induces a pulse voltage in a pick-up coil, which can also be applied for electricity generation as an energy-harvesting element. Dependence of the output voltage on the position of the pick-up coil indicated a fast magnetization reversal by a domain wall propagation. An excitation method for a vibration-type electricity-generating element using a single magnet was optimized by changing the magnet size. The output voltage obtained from the FeCoV wire depended on the amplitude of vibration of an excitation magnet. In order to minimize the vibration amplitude of an excitation magnet required for generating the output voltage, a field distribution from magnets of various sizes was calculated. It was found that just a 0.6 mm-movement of an NdFeB magnet was sufficient to generate the output voltage.

Keywords: magnetic sensor, large Barkhausen jump, FeCoV wire, vibration-type electricity generator, energy harvesting

1. Introduction

A fast magnetization reversal in magnetic wires with bistable states induces a pulse voltage in a pick-up coil. This fast magnetization reversal is accompanied by a large Barkhausen jump, which is known as the Wiegand effect[1]. In this study, a twisted FeCoV wire, one of the optimum materials yielding this effect, was used. A magnetic sensor that uses the Wiegand effect has certain advantages: no external power supply is necessary, and the amplitude of the pulse voltage does not depend on the frequency of an applied magnetic field. This phenomenon has been used in various sensor applications, including speed sensor and rotation sensor[2,3]. In this paper, a vibration-type energy-generating element using the Wiegand effect is reported.

Power generation by environmental vibration is a promising technique for energy harvesting. Vibration-type energy-generating elements, which convert vibration to electricity, mostly have their own eigenfrequency or resonant frequency[4,5]. Vibration at frequency ranges other than specific frequency results in a drastic decrease in electricity generation efficiency[5]. Electricity generation from a vibration-type energy-harvesting element using a FeCoV wire was studied in this paper. The output pulse voltage obtained from the FeCoV wire is expected to be independent of the vibration frequency.

2. Structure of electricity generator

2.1 FeCoV wire

A FeCoV ($Fe_{0.4}Co_{0.5}V_{0.1}$) wire of 0.25 mm diameter and 20 mm length was used in this study. When a torsion stress is applied to the wire, the outer shell near the surface becomes magnetically soft. After releasing the stress, the wire exhibits coercive forces of 20 Oe in the soft layer and 80 Oe in the hard core. Details on magnetic properties of twisted FeCoV wires, including torsion stress dependence, have been reported by Abe *et al.*[6,7]. The magnetic wire shows a uniaxial magnetic anisotropy along its length. The magnetization alignment of the soft layer and the hard core can be in either a parallel state or an antiparallel state, as shown in Figs. 1(a) and (b), respectively.

Figure 2 shows a typical hysteresis loop of the FeCoV wire used in this study, which is essentially the same as that reported in Ref, 6) and 7). The magnetization direction of the soft layer and that of the hard core
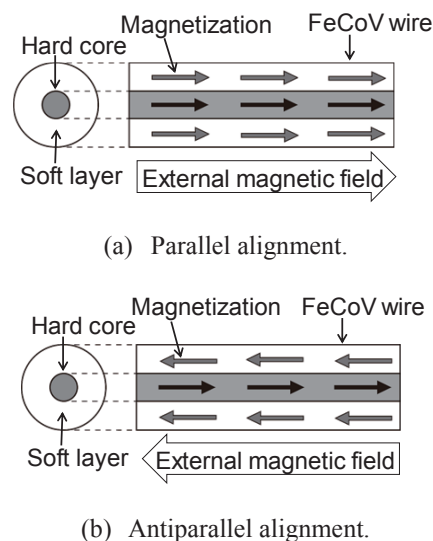

(a) Parallel alignment.

(b) Antiparallel alignment.

Fig. 1 Schematic diagrams of magnetic structure of FeCoV wire with (a) parallel and (b) antiparallel alignments of soft layer and hard core.
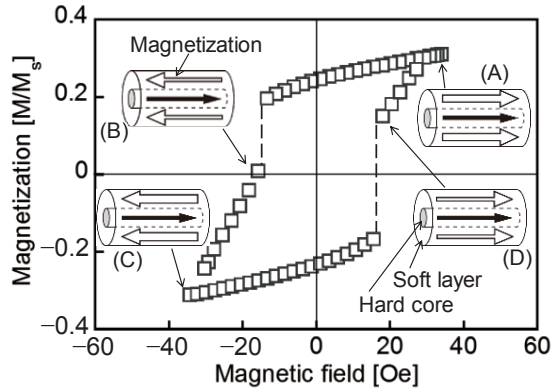
Fig. 2 The measured hysteresis loop of FeCoV wire. A static magnetic field up to 35 Oe was applied.

Fig. 3 Configuration of magnetic wire, magnet, and pick-up coil for electricity generator.

exhibit a parallel state when an external magnetic field larger than 35 Oe was applied along its length, as indicated by (A) in the figure. When a magnetic field with a negative direction reaches −20 Oe, the magnetization of the soft layer is reversed rapidly as indicated by (B). This magnetization reversal, called the Wiegand effect, is due to a fast domain wall propagation. Owing to this magnetization reversal of the soft layer from the parallel state to the antiparallel state, a pulse voltage is induced in a pick-up coil wound around the wire. The magnetization of the soft layer along the left direction is increased by increasing the externally applied magnetic field of the negative direction from −20 Oe (B) to −35 Oe (C). The pulse voltage of the opposite direction is obtained during the magnetization reversal from the antiparallel state (C) to parallel state (D). Within the applied field intensity of ±35 Oe, the magnetization of the hard core is not reversed.

2.2 Vibration of a magnet for electricity generator

A pair of excitation magnets has been conventionally used for repeating the generations of the positive and negative pulse output voltages induced from the wire. In this study, only a single magnet[8] was used to apply a magnetic field of both positive and negative directions to the wire as shown in Fig. 3. This method is advantageous for a vibration-type element in terms of the device structure.

3. Experiment

3.1 Dependence on the position of the excitation magnet

Two pick-up coils of 2 mm length and 50 turns each indicated by Coil 1 and Coil 2 in Fig. 4(a) were wound around the FeCoV wire (diameter: 0.25 mm, length: 20 mm). The output voltage induced in these pickups was measured by changing the position of the excitation NdFeB magnet of $4 \times 4 \times \underline{12}$ mm³ in dimension, where the length of the magnet ($\underline{12}$ mm) is along its magnetization. The underline below the length denotes the magnetization direction of the magnet. The magnet was
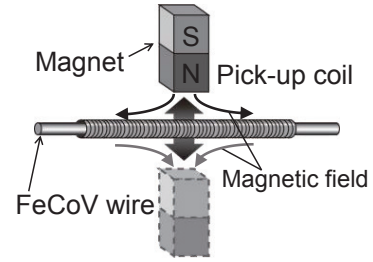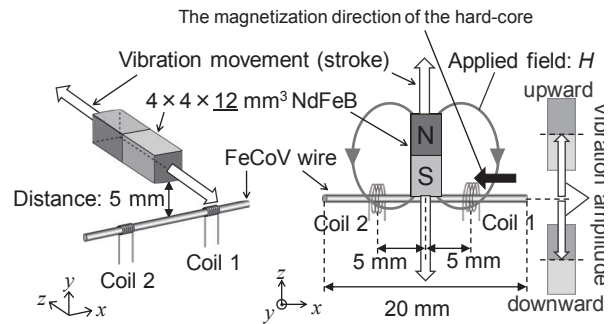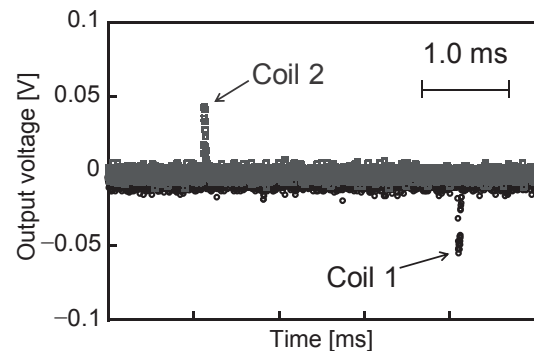

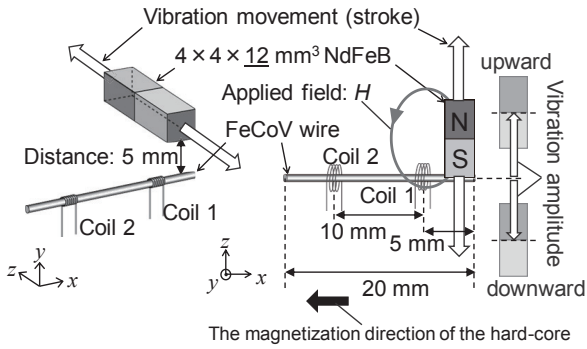(a) Configuration for measurement of induced voltage.

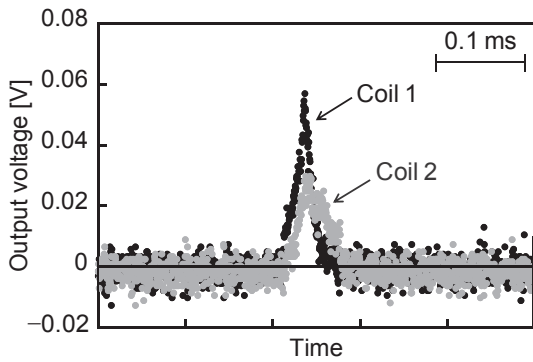(b) Output voltage measured by pick-up coils.

Fig. 4 Configuration of FeCoV wire, pick-up coils, and excitation magnet (a), and waveforms of pulse voltage induced in pick-up coils (b). The excitation magnet was vibrated horizontally at the center of the wire.

vibrated at the center and the end of the wire as shown in Figs. 4(a) and 5(a), respectively. The magnet was vibrated as slow as at 1 Hz. It was confirmed that the output voltage was independent of the vibration frequency.

A vibration amplitude is defined as a length of movement of the vibrated magnet. Each upward or downward movement of the magnet is described as "stroke" in this paper.

(a) Configuration for measurement of induced voltage.

(b) Output voltage measured by pick-up coils.

Fig. 5 Configuration of FeCoV wire, pick-up coils, and excitation magnet (a), and waveforms of pulse voltage induced in pick-up coils (b). The excitation magnet was vibrated horizontally at the end of the wire.

3.2 Dependence on the vibration amplitude of the exciting magnet

The excitation magnet positioned at the end of FeCoV wire (diameter: 0.25 mm, length: 20 mm) was vibrated along the perpendicular direction to the wire, as shown in Fig. 6(a). The output voltages induced in a pick-up coil (1,000 turns and 20 mm length) wound around the wire was measured. The dependence of the output pulse voltage on the vibration amplitude of the magnet was evaluated for various sizes of the excitation magnet.

4. Results and Discussion

4.1 Position of exciting magnet and induced pulse voltage

Figure 4(b) shows the typical waveforms of the pulse voltage induced in the pick-up coils of Coil 1 and 2. These coils were positioned at the right and left sides, 5 mm from the wire center, respectively, as shown in Fig. 4(a). When the excitation magnet was vibrated along the perpendicular direction to the wire, the positive and negative output voltages were induced in Coils 1 and 2, respectively. The amplitude of these two output voltages is almost equivalent. This is because the magnetization
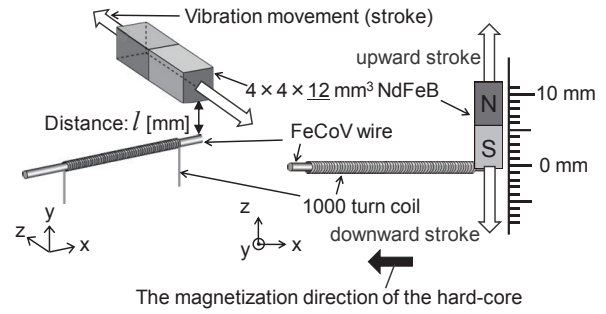
(a) Configuration for measurement of induced voltage.
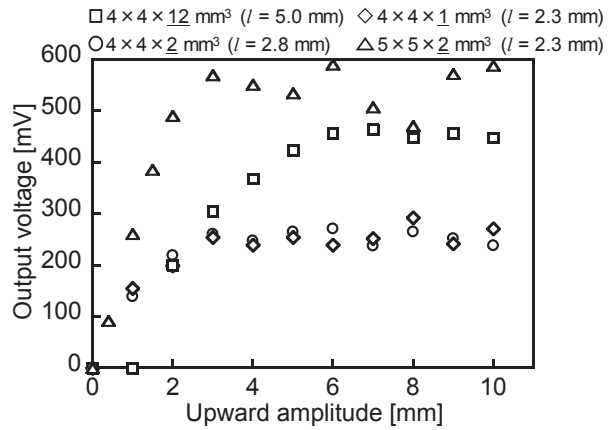
(b) Output voltage measured by pick-up coils.

Fig. 6 Configuration of FeCoV wire, pick-up coil, and excitation magnet (a), and induced output voltages obtained by using various sizes of NdFeB magnets plotted as a function of amplitude of upward stroke.

reversal initiated from the center of the wire, and the magnetization is reversed from the center to both ends of the wire as well as the propagation of the domain wall. On the other hand, when the magnet was vibrated at the end of the wire, the positive output voltages with different amplitudes were induced in Coils 1 and 2, as shown in Figs. 5(a) and 5(b), respectively. This result shows that the magnetization reversal is accompanied by a single domain-wall propagation. The time difference between these two positive pulse voltages agrees with the calculation performed using the distance of the coils and the velocity of the domain wall propagation, which was 500 m/s[9]. The amplitude of the pulse voltage induced in Coil 2 was smaller than that induced in Coil 1. This is because of the energy loss of the domain wall propagation and the smaller amount of reversed magnetization. The intensity of an applied magnetic field from the magnet positioned at the end of the wire was lesser at the position of Coil 2 than it was at that of Coil 1. The full width at half maximum of the pulse voltage induced in Coil 2 was larger than that in Coil 1, which was due to the scattering of the domain

Table 1 Upward amplitudes for their minimum value to obtain the pulse voltage and for giving the saturated voltage, and downward amplitude for generating pulse voltage.

	$4 \times 4 \times \underline{12}$ mm³ ($l = 5$ mm)	$4 \times 4 \times \underline{2}$ mm³ ($l = 2.8$ mm)	$4 \times 4 \times \underline{1}$ mm³ ($l = 2.3$ mm)	$5 \times 5 \times \underline{2}$ mm³ ($l = 2.3$ mm)
Minimum upward amplitude [mm]	2	1	1	0.4
Upward amplitude for saturating output [mm]	6	2	3	3
Downward amplitude for pulse generation [mm]	−1	−0.4	−0.5	−0.2

(a) In the case of upward amplitude is small.
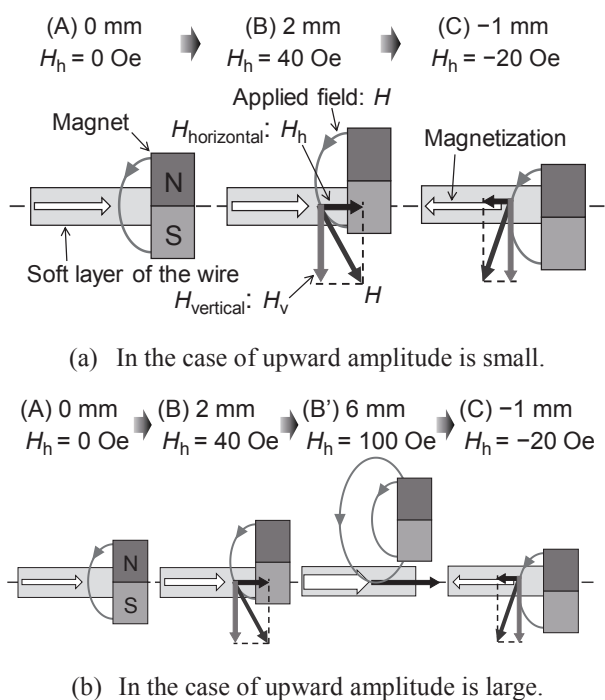
(b) In the case of upward amplitude is large.

Fig. 7 Schematics of positions of the excitation magnet and its magnetic field distribution. A component of the magnetic field along the wire direction is denoted as H_h.

wall propagation at the impurities and defects in the wire.

4.2 Dependence on stroke amplitude of the exciting magnet

Dependence of the output voltage on the vibration amplitude of the excitation magnet is shown in Fig. 6(b). Figure 6(a) illustrates the initial position of the excitation magnet. The vertical distance, l, between the wire and the magnet was 5 mm. The center of the magnet was at 0 mm at the initial position. Then, the magnet was moved upwards as indicated by (A) to (B) in Fig. 7(a). Only the magnetization of the soft layer was shown in all illustrations in Fig. 7. The upward amplitude is 2 mm in case of (B). At this position of the excitation NdFeB magnet of $4 \times 4 \times \underline{12}$ mm³ in dimension, the intensity of the applied magnetic field along the wire direction, noted as H_h in (B) of Fig. 7(b), was 40 Oe.
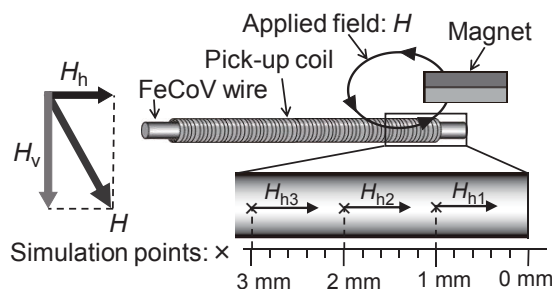

Fig. 8 Schematics indicating H_{h1}, H_{h2}, and H_{h3}, components of a magnetic field from the FeCoV wire along the wire direction. They are the magnetic fields at 1 mm, 2 mm, and 3 mm from the end of the wire.

This field assures the magnetization direction of the soft layer with a positive direction (right side direction in the figure). When the magnet was moved downward from (B) to (C), the pulse voltage was induced in the pick-up coil. The position of the excitation magnet for inducing the pulse voltage was reproducible at −1 mm. H_h was −20 Oe at this position, which agreed with the switching field of the soft layer. This position was independent of the amplitude of the upward stroke of the magnet[10].

Open squares in Fig. 6(b) indicate the output voltage induced at the magnet position of −1 mm as a function of the amplitude of upward stroke of the magnet with $4 \times 4 \times \underline{12}$ mm³ in dimension. It was found that the pulse voltage was obtained if the upward amplitude was 2 mm or larger. The pulse voltage increased with an increase in the upward amplitude, but saturated at 6 mm. The increase and saturation was due to a larger volume of the reversed magnetization of the soft layer and the magnetization saturation of the soft layer, respectively.

### 4.3 Dependence on the magnet dimensions

In order to reduce a vibration amplitude in this electricity-generating element, the output voltage was measured by changing the length of the excitation magnet. The magnets of $4 \times 4 \times \underline{12}$ mm³ ($l = 5.0$ mm), $4 \times 4 \times \underline{2}$ mm³ ($l = 2.8$ mm) and $4 \times 4 \times \underline{1}$ mm³ ($l = 2.3$ mm) for each dimension were used. The vertical distance between the wire and the magnet, l, was adjusted by
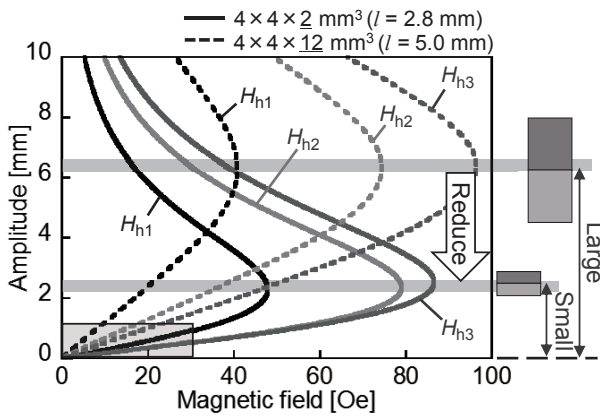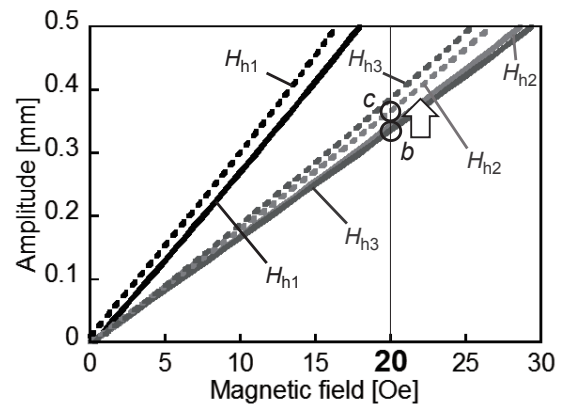
(a) Simulated values of the field intensity.
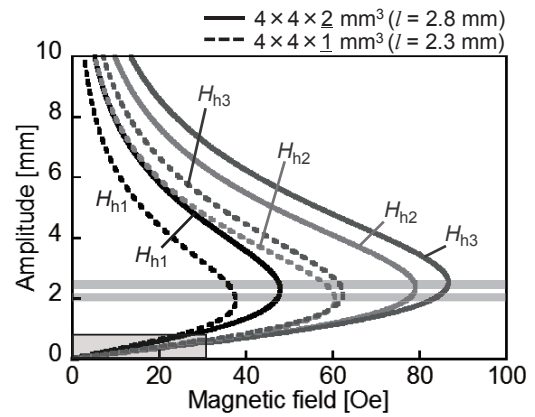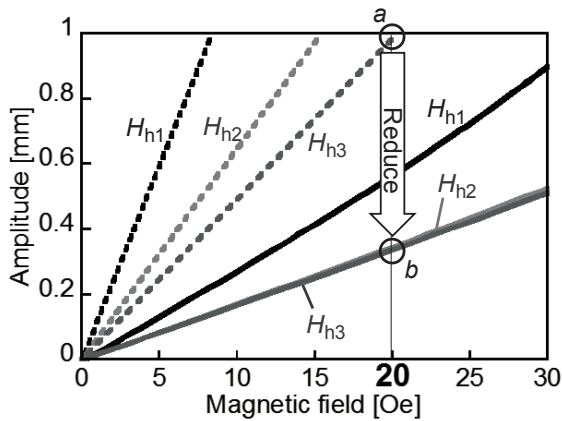
(b) Magnified images of (a) at low magnetic field.

Fig. 9 Magnetic field intensity of component of wire direction, H_h, from NdFeB magnets of $4 \times 4 \times \underline{12}$ mm^3 and $4 \times 4 \times \underline{2}$ mm^3 in dimension calculated as a function of the position of the magnet (equivalent to upward and downward

(a) Simulated values of the field intensity.

(b) Magnified images of (a) at low magnetic field.

Fig. 10 Magnetic field intensity of component of wire direction, H_h, from NdFeB magnets of $4 \times 4 \times \underline{2}$ mm^3 and $4 \times 4 \times \underline{1}$ mm^3 in dimension calculated as a function of the position of the magnet (equivalent to upward and downward amplitudes).

considering the magnet size. The induced pulse voltages measured using these magnets are plotted as a function of the amplitude of the upward stroke in Fig. 6. The magnet of $4 \times 4 \times \underline{2}$ mm^3 could reduce the minimum value of upward amplitude for generating a pulse voltage down to 1.0 mm. The pulse voltage was induced when the position of the magnet was -0.4 mm. This result shows that electricity can be generated by a vibration of 1.4 mm (upward 1.0 mm + downward -0.4 mm) of the magnet.

In order to understand this dependence on magnet size, the magnetic field distribution was calculated using a commercial software (JMAG distributed by JSOL Corporation). The magnetic field intensity along the wire directions, H_{h1}, H_{h2} and H_{h3}, were calculated, which are the magnetic fields at 1 mm, 2 mm and 3 mm from the wire end, respectively, as shown in Fig. 8. As the FeCoV wire exhibits strong uniaxial anisotropy

along the wire direction, the wire-direction component of the applied magnetic field is essential to discuss the magnetization reversal of the wire. The numerical analysis based on the field intensities of H_{h1}, H_{h2} and H_{h3} was sufficient to discuss the experimental results, as described afterwards.

Figure 9 shows the simulated values of the field intensity of the $4 \times 4 \times \underline{12}$ mm^3 and the $4 \times 4 \times \underline{2}$ mm^3 magnets as a function of the position of the magnet while vibrating in the upward/downward directions. The position of the magnets at of 6 mm and 2 mm for giving the maximum magnetic field intensities of H_{h1}, H_{h2} and H_{h3} from the $4 \times 4 \times \underline{12}$ mm^3 and the $4 \times 4 \times \underline{2}$ mm^3 dimensions, respectively, as shown by gray lines in Fig. 9(a) agreed with the upward amplitudes at which the increase in output voltage was saturated for each magnet.

Figure 9(b) is a magnified image of Fig. 9(a) for the
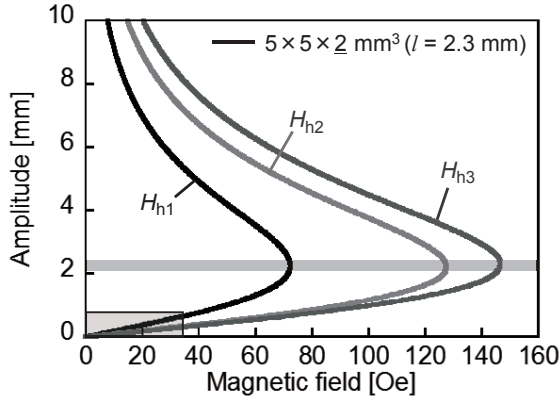
(a) Simulated values of the field intensity.
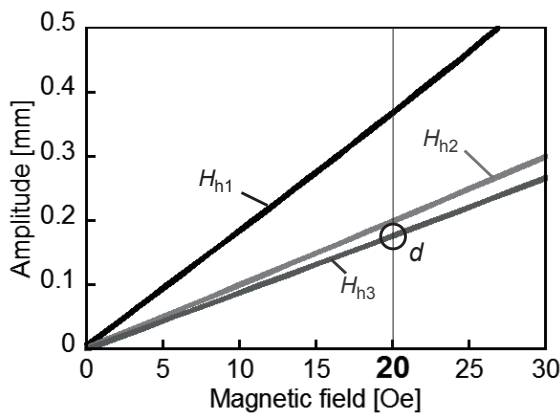
(b) Magnified images of (a) at low magnetic field.

Fig. 11 Magnetic field intensity of component of wire direction, H_h, from NdFeB magnet of $5 \times 5 \times \underline{2}$ mm³ in dimension calculated as a function of the position of the magnet (equivalent to upward and downward amplitudes).

magnetic field range of 0–30 Oe. The positions for the applied magnetic field of 20 Oe, which is a switching field of soft layer, are calculated to 1.0 mm and 0.4 mm for the $4 \times 4 \times \underline{12}$ mm³ and $4 \times 4 \times \underline{2}$ mm³ magnets, respectively. These positions noted by circles (a) and (b) in the figure agree with the downward amplitudes of the magnet for generating the pulse voltage due to the magnetization reversal of the soft layer. Table 1 summarizes these specific upward and downward amplitudes theoretically supported by the simulation of the magnetic field distribution.

Figure 6(b) also shows the output voltage dependence on the upward amplitude of an $4 \times 4 \times \underline{1}$ mm³ magnet. The experimental results indicate that the output properties using $4 \times 4 \times \underline{2}$ mm³ and $4 \times 4 \times \underline{1}$ mm³ magnets are similar. This is also confirmed by the calculated results shown by Fig. 10(a) and 10(b). The positions of the magnets for the maximum magnetic field and for applying 20 Oe were not different between in the two magnets, as

indicated by circles (b) and (c) in Fig. 10(b).

A magnetic field intensity of H_{h1} is smaller than those of H_{h2} and H_{h3} as shown in Figs. 9 and 10. This is because that the direction of the magnetic field at 1 mm from the edge of the wire is close to perpendicular to the wire direction, and that H_{h1}, the wire-direction component of the applied magnetic field, is small. The magnetization reversal of the wire is initiated by the applied field of H_{h2} and H_{h3}.

Finally, the output property with the optimized magnet dimension and distance between the wire and the magnet is reported. Figure 6(b) shows the output voltage measured using an NdFeB magnet of $5 \times 5 \times \underline{2}$ mm³ ($l = 2.3$ mm) in dimension. Figure 11 shows the simulated values of the field intensity of this magnet. The output voltage was as large as 600 mV. The minimum value of the upward amplitude for generating pulse voltage was as small as 0.4 mm. The pulse voltage was induced when the downward amplitude was 0.2 mm. This agreed with the calculated amplitude for reversing the magnetization of the soft layer, indicated by circle (d) in Fig. 11(b). It was found that the electricity generation can be obtained by a vibration of 0.6 mm (upward 0.4 mm + downward −0.2 mm) of the magnet. These values for upward and downward amplitudes, which are summarized in Table 1, are mostly consistent with the simulated result of a magnetic field distribution, as shown in Figs. 9, 10 and 11.

5. Conclusion

This paper proposes a vibration-type electricity generator using a FeCoV wire. The pulse voltage was induced in a pick-up coil wound around the wire by vibrating an excitation magnet. The induced output voltage was attributed to a fast magnetization reversal of the wire known as the Wiegand effect. Dependence of the output voltage on the position of a pick-up coil indicated a fast magnetization reversal by a domain wall propagation. An excitation method using a single magnet for a vibration-type electricity-generating element was optimized by changing the size of the excitation magnet. The minimum amplitude of vibration of the excitation magnet required to obtain the output voltage strongly depended on the dimension of the magnets, which agreed well with the calculated results of a field distribution from the magnets. It was found that even a 0.6 mm-movement of the NdFeB magnet of $5 \times 5 \times \underline{2}$ mm³ in dimension could generate a pulse voltage.

References

1) J. R. Wiegand and M. Velinsky: U.S. Patent #3,820,090 (1974).
2) R. Malmhall, K. Mohri, F. B. Humphrey, T. Manabe, H.

Kawamura, J. Yamasaki and I. Ogasawara, *IEEE Trans. Magn.*, **23**, 3242 (1987).

3) M. Vázquez, C. Gómez- Polo, D.-X. Chen and A. Hernando, *IEEE Trans. Magn.*, **30**, 907 (1994).

4) A. Moure, M.A. Izquierdo Rodríguez, S. Hernández Rueda, A. Gonzalo, F. Rubio-Marcos, D. Urquiza Cuadros, A. Pérez-Lepe, J.F. Fernández, Energ. *Convers. Manage.*, **112**, 246 (2016).

5) V. Ostasevicius, V. Markevicius, V. Jurenas, M. Zilys, M. Cepenas, L. Kizauskiene, V. Gyliene, *Sensor Actuat. A-Phys.*, **233**, 310 (2015).

6) S. Abe and A. Matsushita, *IEEE Trans. Magn.*, **31**, 3152 (1995).

7) S. Abe, A. Matsushita, and M. Naoe, *IEEE Trans. Magn.*, **33**, 3916 (1997).

8) T. Kohara, T. Yamada, S. Abe, S. Kohno, F. Kaneko and Y. Takemura, *J. Appl. Phys.*, **109**, 07E531-1 (2011).

9) H. Tanaka, T. Yamada, Y. Takamura, S. Abe, S. Kohno and H. Nakamura, *IEEE Trans. Magn.*, **43**, 2397 (2007).

10) A. Takebuchi, N. Kameda, T. Yamada, Y. Takemura, 2016 Joint MMM-Intermag Conference, DJ-02, San Diego, Jan, 2016.